# New Algorithm for Automated Snow Cover Monitoring and Understanding Impact of Topographic Influence on Sub-pixel Analysis Using AWiFS - II on Himalaya

Priyanka Handa[*], V.D. Mishra[**], J.K. Sharma[*]

[*]*Rayat Institute of Engineering & Information Technology,S.B.S.Nagar,Punjab 144533 ,India*

[**]*Snow and Avalanche Study Establishment , Defense Research and Development Organization,Chandigarh 160 036 , India .*

## *Abstract*

*Snow cover information is very important for many applications. Therefore, it is necessary to calculate this information as accurately as possible. In this paper, the sub pixel classification technique namely linear unmixing method has been applied on topographically uncorrected and corrected reflectance images. But this method doesnot filter snow under shadow. It is attempted to develop a new algorithm with the help of NDSI and subpixel quantification which offers more improved information without assuming any threshold. It is found that the fractional snow cover within an AWiFS- II pixel using this approach is provided with root mean square error of less than 0.1 over the range from 0.0 to 1.0. The comparative analysis of both topographic corrections and their reverse shows that the root mean square error is decreasing and co-relation coefficient ($r^2$) is increasing after applying topographic corrections. Which shows that topographic corrections can provide more detailed and improved snow cover information.*

**Keywords:** Advance Wide Field Sensor (AWiFS-II), Subpixel, Topographic Corrections.

## 1. Introduction

Knowing the extent of snow is an important parameter for various hydrological, climatological and snow hazard applications. It affects the hydrological and climatological cycle as the amount of water extract from snow melt affects the water supply systems, floods, water use, and waste water in urban areas, aquatic ecosystems management, water trading and virtual water [1]. Snow feedback is also related to global warming (caused by increasing concentrations of atmospheric green house gases) as warmer earth will have less snow cover, resulting in a darker planet that absorbs more solar radiation. Also, the large snow cover areas can cause formation of avalanches which is destructive for life [2]. Snow cover monitoring can be done with the help of many methods like Normalized Difference Snow Index (NDSI), Normalized Difference Channel index (NDCI), S3 [3] but these techniques have some drawbacks [4] as snow in a pixel with these techniques can be identify on the basis of their threshold and snow cover ratio percentage (SCR %) . It is found that NDSI , NDCI and S3 has snow cover ratio percentage of 50 % ,60% and 55% respectively which demonstrates the pixel is either snow covered or not on the basis of snow cover percentage in it [3]. However, there is a need to know the fractional snow cover and its distribution as accurately as possible. In this paper, it is attempted to develop a new algorithm for snow cover information using AWiFS-II sensor on RESOURCESAT-2 without any assumption. A subpixel classification technique namely linear unmixing method has been implemented which differentiates different land scapes. But this classification technique does not retrace snow under shadow. Therefore, regression relationships are developed between the normalized difference snow index (NDSI) and the fraction of snow cover area of multi-temporal AWiFS-II images. In addition to this, topographic corrections [5] [6] are also applied on reflectance images of various AWiFS-II scenes. Automatic snow cover retrieval algorithm without any threshold assumption is developed for both topographically corrected and uncorrected images thus finds the suitability of different algorithms for accuracy.

## 2. Study area

The study area is extending from latitude 31° 30' 00" N to 33° 30' 00" N and longitude 76° 30' 00" E to 78° 00' 0" E. Mean elevation of the area is in between 4000 m and 4500 m and slopes vary from $0^o$ to $88^o$. Majority of the slopes have eastern and southern aspects. In between 2400 and 3100 m altitude, densely forested area is present. It is scanty beyond 3100m. However, below 2400m, area is habituated. Intense wind activities with moderate to heavy snow fall generally occurs above 2400m within this area.

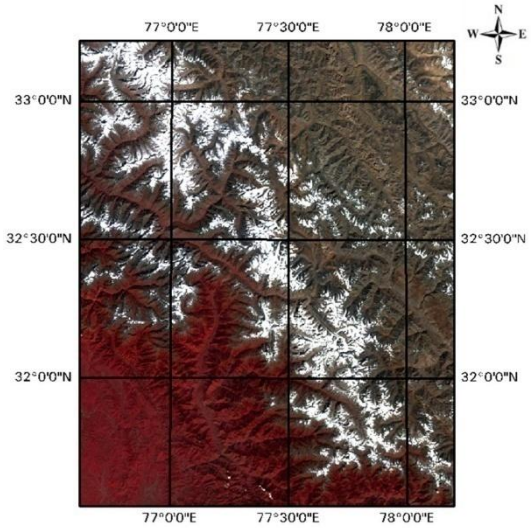


**Figure 1. Study area of AWiFS-II image**

## 3. Satellite data

Almost cloud free multi-temporal satellite images of AWiFS-II from October 2011 to March 2012 are used in the present work to understand the impact of topographic correction and to develop a new algorithm. The salient specifications of AWiFS II sensor are given in the Table 1.

## 4. Methodology

### 4.1. DN (Digital Number) image

Each image element (pixel) is described by a meaningful digital number (DN). DN reflects radiation value, reflected by the earth surface and measured by a sensor. These radiances measured in spectral wavelength region are converted to Digital Numbers (DNs) for the sake of storage and data transfer convenience. Thus received satellite image is delivered as an image of raw digital number (DN) values. DN for a single pixel can be written using 8 to 24 bits depending on radiometric resolution of the sensor.[7][8]

### 4.2. Radiance image

Any spectral index can't apply to this raw data (whether topographic correction or any other measure) as DN values have no unit and any physical connotation. Therefore, there is needed to be converted (DN values) to radiance, then to at- sensor (top-of-atmosphere) reflectance and further to surface reflectance in order to draw quantitative analysis from remote sensing data. Spectral Radiance in $mW/cm^2/sr/\mu m$ [5][9][10] is estimated using the following equation.

$$L_\lambda = \frac{DN}{DN_{max}}(L_{max} - L_{min}) + L_{min}, \qquad (1)$$

Where, $L_\lambda$ = spectral radiance at the sensor's aperture, DN = input digital number image, $DN_{max}$ = maximum digital number, $L_{max}$= maximum radiance value, $L_{min}$= minimum radiance value which is zero for AWiFS-II

### 4.3. Image geo-referencing and DEM

All the AWiFS-II sensor images were geo-referenced using master image of the study area. The master image was generated after rectification with 1:50,000 toposheet. The images were orthorectified using digital elevation model (DEM) and projective transform geometric model available in ERDAS IMAGINE 9.1. All the satellite images were geocoded to the Everest datum. The accuracy of geo-referencing of all satellite images were less than a pixel. ASTER (Advanced Spaceborn Thermal Emission and Reflection Radiometer) DEM available free was used with 30 m spatial resolution. The grid resolution of DEM was further resampled to 56 m equal to spatial resolution of AWiFS-II. The DEM was further used to derive terrain parameters slope, aspect and illumination angle for topographic corrections.

### 4.4. Reflectance without topographic corrections

The spectral reflectance of each AWiFS-II band was derived directly from the satellite data using atmospheric corrected radiance, without any terrain correction in equation (2)

$$R_\lambda = \frac{\pi(L_\lambda - L_p)d^2}{t_v(E_0 \cos\theta_z t_z + E_d)}, \qquad (2)$$

Where, $R_\lambda$ is the reflectance of a pixel in a particular band, $L_\lambda$ is at satellite spectral radiance from pixel in each band ($mW/cm^2/sr/\mu m$), $L_p$ is the path radiance, d is the earth sun distance in

**Table 1. Salient specifications AWiFS-II sensor**

| Spectral bands | Spectral wavelength(nm) | Spatial resolution(m) | Quantization(bit) | Maximum radiance ($mw/cm^2/sr/\mu m$) | Solar exoatmospheric spectral irradiance ($mw/cm^2/sr/\mu m$) |
|---|---|---|---|---|---|
| B2 | 520-590 | 56 | 12 | 52.34 | 185.3281 |
| B3 | 620-680 | 56 | 12 | 40.75 | 158.042 |
| B4 | 770-860 | 56 | 12 | 28.425 | 108.357 |
| B5 | 1550-1700 | 56 | 12 | 4.645 | 23.786 |

astronomical units (AU), $E_0$ is the bandpass exoatmospheric spectral irradiance (Table1), $E_d$ is the downwelling spectral irradiance.It is assumed to be equal to zero. $\theta_z$ is the solar zenith angle(degree), $t_v$ is the transmittance in the atmosphere from ground surface to sensor and $t_z$ is the transmittance in the atmosphere from Sun to ground [5].

### 4.5. Reflectance with topographic corrections

Topographic corrections are a necessary step in remote sensing applications in areas of high relief. As, in these type of terrains, topographic variability like steep and varying slopes causes differential illumination problem. Thus hampered the remote sensing applications of these terrains. In the present study, slope matching technique is used for topographic corrections which are best suitable for Himalayan terrain according to [5]. Topographically corrected reflectance is demonstrated as [5][6][11]:

$$R_{n\lambda ij} = R_{\lambda ij} + (R_{max} - R_{min}) * \frac{\left[\left(\langle \cos i \rangle s - \cos_{ij} i\right)\right] C_\lambda}{\langle \cos i \rangle s}, \quad (3)$$

where, Rnλij is the normalized reflectance values for image pixel ij in wave band λ, $R_{\lambda ij}$ is the uncorrected original reflectance on the tilted surface for image pixel ij in wave band λ, $\cos_{ij} i$ is illumination (IL) image for each pixel ij of the study area , ‹cosi›s is the mean value of illumination on the south aspect rather than the overall mean of the entire image, Rmax and Rmin are the maximum and minimum reflectance values of the land cover in uncorrected image. The advantage of this method is that the reflectance values in the corrected image are normalized to the mean illumination level of pixels on the sunny aspect rather than the overall mean illumination Value of the entire image. $C_\lambda$ is the correction coefficient in different wavelength bands, λ, , and determined using the difference of reflectance values between sunlit and shady slopes with the uncorrected and first stage normalized image uncorrected and first stage normalized image using the following equation:

$$C_\lambda = \frac{S'_\lambda - N_\lambda}{N'_\lambda - N_\lambda}, \quad (4)$$

Where, $S'_\lambda$ is the mean reflectance value on sunlit slopes after first stage normalization, $N_\lambda$ is the mean reflectance value on shady slopes in uncorrected image and $N'_\lambda$ is the mean reflectance value on shady slopes after first stage normalization.

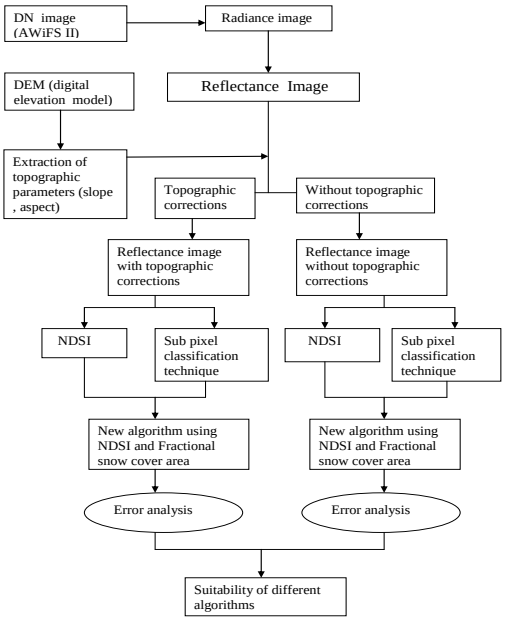


**Figure 2. Flow chart for methodology**

### 4.6. NDSI

Normalized Difference Snow Index (NDSI) is the difference of two bands (one in visible and one in the near infrared or short wave infrared parts of the spectrum ) and used to map snow[12][13][14]. Snow is highly reflective in the visible part of the electromagnetic spectrum and highly absorptive in

the near – infrared or short wave infrared parts of the spectrum. NDSI is defined as:

$$\text{NDSI} = \frac{R_{GREEN} - R_{SWIR}}{R_{GREEN} + R_{SWIR}}, \qquad (5)$$

Where, $R_{GREEN}$ and $R_{SWIR}$ are reflectances in green and SWIR bands. AWiFS - II green band is Band 2 having wavelength 520nm – 590nm and SWIR band is band 5 having wavelength 1550 nm – 1700 nm. To differentiate the non snow and snow covered area in a pixel, a threshold value of 0.4 is defined here for the pixels that are approximately 50% or greater covered by snow from the imageries of different sensors.

### 4.7. Sub-pixel

Subpixel classification technique is used to estimate the precise distribution of snow class fractions from medium/moderate spatial resolution images as the data provided from various sensors brings the problem of mixed pixels. In the present study, three classes' snow, vegetation and soil are identified using a sub-pixel classification technique. The pure training sites for these three classes are extracted using visual analysis and spectral reflectance characteristics.

### 4.8. Sub-pixel model

Linear unmixing method has been implemented for subpixel snow cover mapping. It is used for solving the mixed pixel problem. The hypothesis underlying linear unmixing is that the spectral radiance measured by the sensor consists of the radiances reflected by all of these materials, summed in proportion to the subpixel area covered by each material. The response of each pixel in any spectral wavelength can be considered as a linear combination of the responses of each component, which are assumed to be in the mixture. Hence, in multispectral image, it is possible to model each pixel spectrum of the image as a linear combination of a finite set of components:

$$r_1 = a_{11*x1} + a_{12*x2} + \cdots + a_{1n*xn} + e_1, \quad (6)$$

$$r_2 = a_{21*x1} + a_{22*x2} + \cdots + a_{2n*xn} + e_2, \quad (7)$$

$$r_m = a_{m1*x1} + a_{22*x2} + \cdots + a_{mn*xn} + e_m \quad (8)$$

In generalized form these equations can be written as

$$r_i = \sum_{j=1}^{n}(a_{ij} * x_j) + e_i \qquad (9)$$

where, $r_1$ is spectral response of the pixel in ith spectral band, $a_{ij}$ is spectral response of the jth component in the pixel for ith spectral band, $x_j$ is proportion value of the jth component in the pixel, $e_i$ is error term for the ith spectral band. This error is due to the assumption made that the response of each pixel in any spectral wavelength is a linear combination of the proportional responses of each component.j = 1,2,3….n (number of components assumed for the problem =3), i= 1,2,3….m (number of spectral bands used in problem = 4).

### 4.9. Development of new algorithm

Subpixel classification technique cannot retrace snow under shadow [3][5]. So, a new statistical relationship is developed between the NDSI and the fraction of snow cover for the topographically uncorrected and corrected reflectance. The algorithm has been developed with the help of regression relationships between the NDSI and fraction of snow cover for various AWiFS-II scenes. The generalized new algorithms from multiple regression equation for topographically uncorrected and corrected images are given below:

Without topographic corrections:

$$Y = 0.755\ X + 0.0712, \qquad (10)$$

With topographic corrections :

$$Y = 0.928\ X + 0.0782, \qquad (11)$$

Where Y is fractional snow cover and X represents NDSI image.

### 4.10 Error analysis

Classification is not complete unless error analysis has been performed. The root mean square error (RMSE) is calculated using equation (9) as follows [2]:

$$\text{RMSE} = \sqrt{\frac{1}{m}\sum_{1}^{m} e_i^2} \qquad (11)$$

Where $e_i^2$ is squared error as mentioned in equations (6-8) and m are number of bands.

## 5. Results and discussions

In the present work, sub pixel classification namely linear unmixing method is applied on both topographically uncorrected and corrected reflectance images of various AWiFS-II scenes which works upon the hypothesis that the spectral radiance measured by the sensor consists of the radiance reflected by all of these materials, summed in proportion to the subpixel area covered by each material. Thus, it extracts different classes of landcovers on the basis of this hypothesis. In the

present study, three classes are extracted namely snow, soil and vegetation with respect to their spectral signature. However, the studies have been done only on the snow covered area extracted. Figure 3, shows the resulted outcome of the snow fraction using subpixel classification technique.

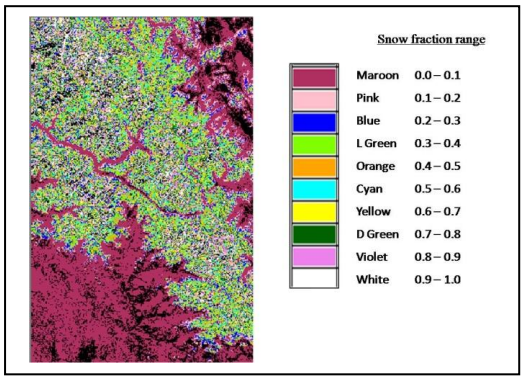


**Figure 3. Snow fraction resulted from the subpixel classification technique**

But subpixel classification technique cannot retrace snow under shadow. To filter the snow under shadow portion, regression relationship is developed with the help of NDSI image and snow fraction image resulted from the subpixel classification technique. Figure 4 and 5, shows the regression relationship developed for one of the AWiFS-II imageries

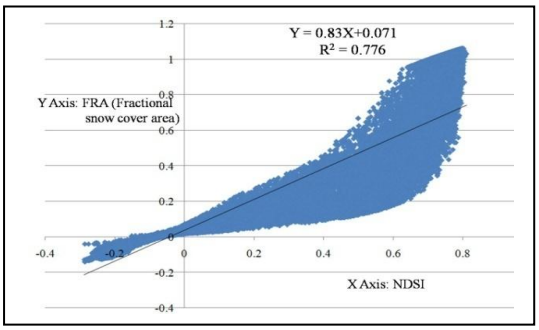


**Figure 4. Regression relationship developed for AWiFS II (13 november 2011) imagery, without topographic corrections between NDSI image and fractional snow, extracted using subpixel classification technique.**

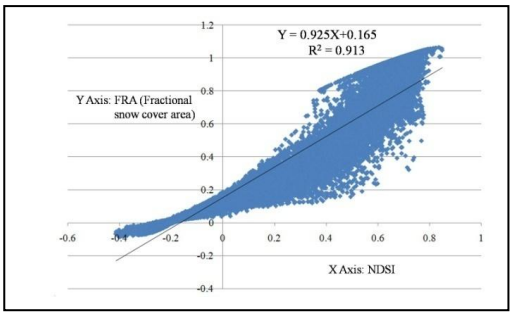


**Figure 5. Regression relationship developed for AWiFS II (13 november 2011) imagery, with topographic corrections between NDSI image and fractional snow, extracted using subpixel classification technique.**

Similarly various statistical relationships have been developed. Table 2 shows various regression relationships of different AWiFS-II imageries.With the help of these relationships, generalized algorithms for both (topographically uncorrected and corrected results) have been developed as given in the equations (10,11).

The robustness of the algorithm can be estimated from its correlation coefficient (which is above 0.6 in most of the cases, table 3 shows the correlation coefficients) and root mean square error (which is less than 0.1 over the range of 0 to 1). Table 4 shows the root mean square errors of sub-pixel analysis. It can be interpreted from the table 3 and table 4 that inclusion of topography improves correlation and minimize root mean square error.

**Table 2. Regression relationships for various AWiFS-II imageries between NDSI and fractional snow area extracted using subpixel classification technique, where X is NDSI and Y is the fractional snow cover area**

| Regression relationships | | |
|---|---|---|
| Imagery dates | Without topographic corrections | With topographic corrections |
| 15 October 2011 | Y=0.650X+0.113 | Y=0.726X+0.150 |
| 24 October 2011 | Y=0.815X+0.036 | Y=0.995X+0.007 |
| 13 November 2011 | Y=0.83X+0.071 | Y=0.925X+0.165 |
| 17 November 2011 | Y=0.698X+0.074 | Y=0.896X+0.045 |
| 27 November 2011 | Y=0.614X+0.100 | Y=0.760X+0.091 |
| 11 December 2011 | Y=0.630X+0.057 | Y=0.843X+0.024 |
| 16 December 2011 | Y=0.794X+0.027 | Y=1.023X-0.032 |
| 17 December 2011 | Y=0.843X+0.052 | Y=0.993X+0.041 |
| 21 December 2011 | Y=0.813X+0.098 | Y=1.151X-0.024 |
| 24 January 2012 | Y=1.217X-0.157 | Y=1.329X-0.113 |
| 29 January 2012 | Y=1.349X-0.275 | Y=2.559X-0.902 |
| 17 February 2012 | Y=1.618X-0.358 | Y=1.580X-0.221 |
| 26 February 2012 | Y=1.457X-0.263 | Y=1.660X-0.306 |
| 02 March 2012 | Y=1.018X-0.049 | Y=1.258X-0.139 |

**Table 3. Correlation coefficients ($R^2$) between NDSI and sub-pixel snow fraction**

| Correlation coefficient ($R^2$) | | |
|---|---|---|
| Imagery dates | Without topographic corrections | With topographic corrections |
| 15 Oct 2011 | 0.849 | 0.901 |
| 24 Oct 2011 | 0.678 | 0.789 |
| 13 Nov 2011 | 0.776 | 0.913 |
| 17 Nov 2011 | 0.747 | 0.837 |
| 27 Nov 2011 | 0.793 | 0.872 |
| 11 Dec 2011 | 0.669 | 0.792 |
| 16 Dec 2011 | 0.825 | 0.920 |
| 17 Dec 2011 | 0.907 | 0.945 |
| 21 Dec 2011 | 0.789 | 0.885 |
| 24 Jan 2012 | 0.495 | 0.552 |
| 29 Jan 2012 | 0.556 | 0.893 |
| 17 Feb 2012 | 0.393 | 0.446 |
| 26 Feb 2012 | 0.559 | 0.621 |
| 02 March 2012 | 0.627 | 0.749 |

**Table 4. RMSE of sub-pixel analysis**

| Root mean square error (RMSE) | | |
|---|---|---|
| Imagery dates | Without topographic corrections | With topographic corrections |
| 15 Oct 2011 | 0.06 | 0.05 |
| 24 Oct 2011 | 0.04 | 0.03 |
| 13 Nov 2011 | 0.08 | 0.07 |
| 17 Nov 2011 | 0.08 | 0.07 |
| 27 Nov 2011 | 0.07 | 0.06 |
| 11 Dec 2011 | 0.09 | 0.05 |
| 16 Dec 2011 | 0.07 | 0.05 |
| 17 Dec 2011 | 0.06 | 0.04 |
| 21 Dec 2011 | 0.08 | 0.06 |
| 24 Jan 2012 | 0.1 | 0.08 |
| 29 Jan 2012 | 0.099 | 0.097 |
| 17 Feb 2012 | 0.1 | 0.07 |
| 26 Feb 2012 | 0.09 | 0.08 |
| 02 March 2012 | 0.08 | 0.07 |

## 6. Conclusion

In the present study, it is examined that NDSI is found useful in estimating the fractional snow cover within an AWiFS-II pixel. A statistical relationship has been developed between NDSI and fractional snow cover area extracted using linear unmixing method. The root mean square error and correlation coefficient shows that the algorithm is robust and automated. The results show that the fractional snow area within an AWiFS-II pixel can be provided with a root mean square error of less than 0.1 over the range of 0.0 to 1.0. In adition to this, topographic corrections are also applied and a comparative analysis has been done between both. This analysis shows that the correlation coefficient is increasing and root mean square error is decreasing after applying topographic corrections. The new algorithm will ignore the problem of assuming threshold for NDSI used for quantitative estimation of snow cover.

## Acknowledgements

The authors are thankful to Sh. Ashwagosha Ganju, Director, Snow and Avalanche Study establishment (SASE) to grant permission to pursue M.Tech project in Remote Sensing Research Group. Authors also heartly wish to thank Sh.. Himanshu, Sh. Gurusewak Singh Brar, Sh. Vaibhav Sharma, Sh. Shiva Reddy, Sh. Sahil sood and Sh.. Avinash Negi for their help and encouragement.

## References

[1] A. Ghandhari and S.M.R. Alavi Moghaddam, Water balance principles: A review of studies on five watersheds in Iran, Journal of Environment Science and Technology 4(5): 2011, 465-479.

[2] K. Jagjit Sharma, Puneeta, D. Varunendra Mishra, New algorithm development for snow cover monitoring at sub pixel level using MODIS data, Atti Della" Fondazione Giorgio ronchi" , ANNO, LXV-N.4, 2010, 440-452 .

[3] Devesh Khosla, J.K. Sharma, V.D. Mishra, Snow cover monitoring using different algorithm on AWiFS sensor Data, International Journal of Advanced Engineering Sciences and Technologies, Vol No. 7, Issue No. 1, 2011, 042-047.

[4] V.V. Salomonson, I. Appel, Estimating fractional snow cover from MODIS using the normalized difference snow Index, Remote Sensing of Environment 89, 2004, 351-360.

[5] V.D. Mishra, J.K. Sharma, K.K Singh, N.K Thakur and M Kumar, Assessment of different topographic corrections in AWiFS satellite imagery of Himalaya terrain, J.Earth Syste. Sci 118, No. 1, February 2009, pp. 11-26.

[6] P. Fureder, Topographic Correction of Satellite images for improved LULC classification in Alpine Areas, Grazer Schriften der Geographie und Raumforschung, band 45, 2010, pp-187-194.

[7] Wanxiao Sun, Photogrammetric Engineering and Remote sensing, vol.72, No.4, April 2006, 373-382

[8] Murugan S, Jothi Venkateswaran C, Radhakrishnan N, Extraction of linear objects and features from remote sensing image (RSI) using edge detection algorithms , Indian J. Edu. Inf. Manage, vol.1, No.5(May 2012)

[9] Song C, Woodcock C E, Seto K C, Lenney M P and Macomber AS 2001, Classification and change detection using Landsat TM data: when and how to correct atmospheric effects; Remote Sensing Environment.75, 2001, 230-244.

[10] Pandya M R, Singh R P, Murali K R, Babu P N, Kiran kumar A S and Dadhwal V K, Band pass solar exo-atmospheric irradiance and Rayleigh optical thickness of sensors on board, Indian remote sensing satellites-1B,-1C,-1D and P4; IEEE trans. Geosci. Remote Sens. 40(3), 2002, 714-717.

[11] Nichol J, Hang L K and Sing W M, Empirical Correction of low Sun angle images in steeply sloping terrain; a slope matching technique, Int J. Remote Sens. 27(3-4), 2006, 629-635.

[12] H.S. Negi, A.V. Kulkarni and B.S. Semwal, Estimation of snow cover distribution in Beas Basin ,Indian Himalya using satellite data and ground measurement, Journel of Earth System Science, 118, No.5, October 2009, 525-538.

[13] S. Subramaniam, A.V. Suresh Babu, E . Sivasankar, V. Venkateshwar Rao and G. Behera , Snow Cover Estimation from Resourcesat-1 AWiFS-Image Processing with an Automated Approach, International Journal of Image Processing (IJIP), Volume(5), Issue(3), 2011, 298-320.

[14] Sanjay K Jain, A K Lohani and R O Singh, Snowmelt Run Off Modelling in a basin located in Bhutan Himalaya, India Water Week 2012 –Water, Energy and Food Security: Call for Solutions, New Delhi, 10-14 April 2012.